A

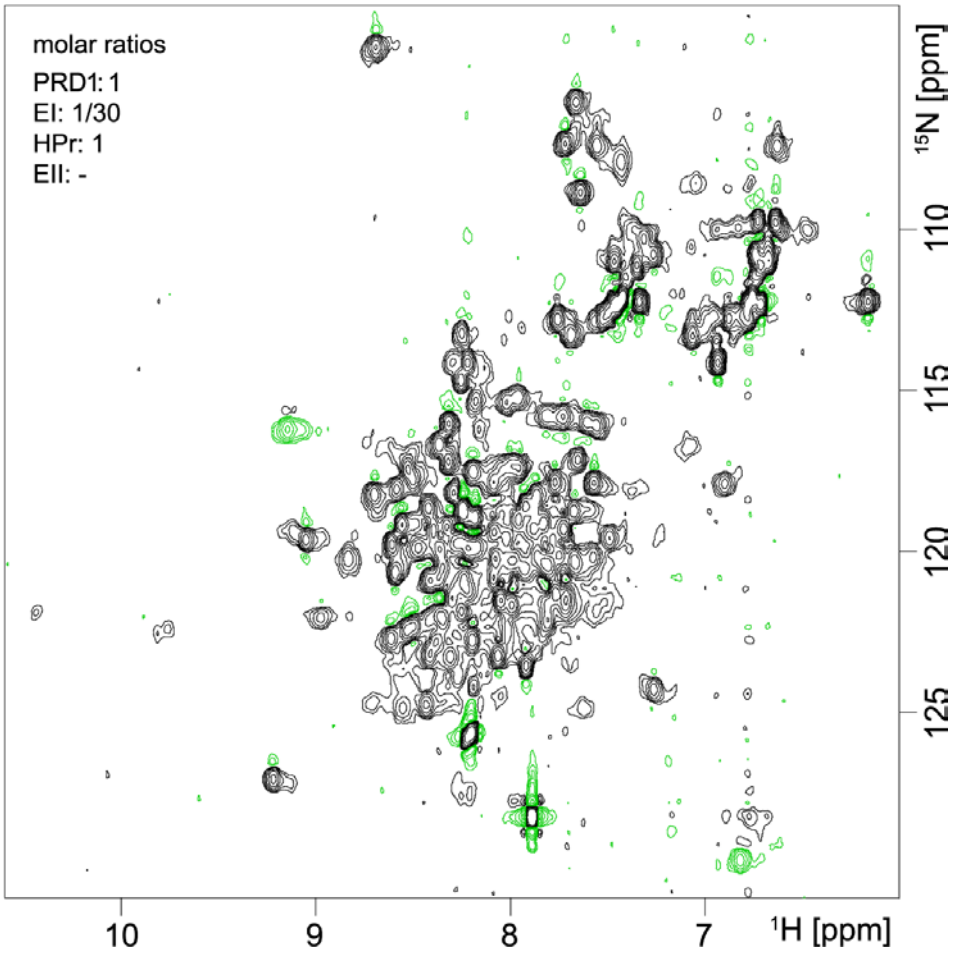

Himmel et al. Fig. S1a

B

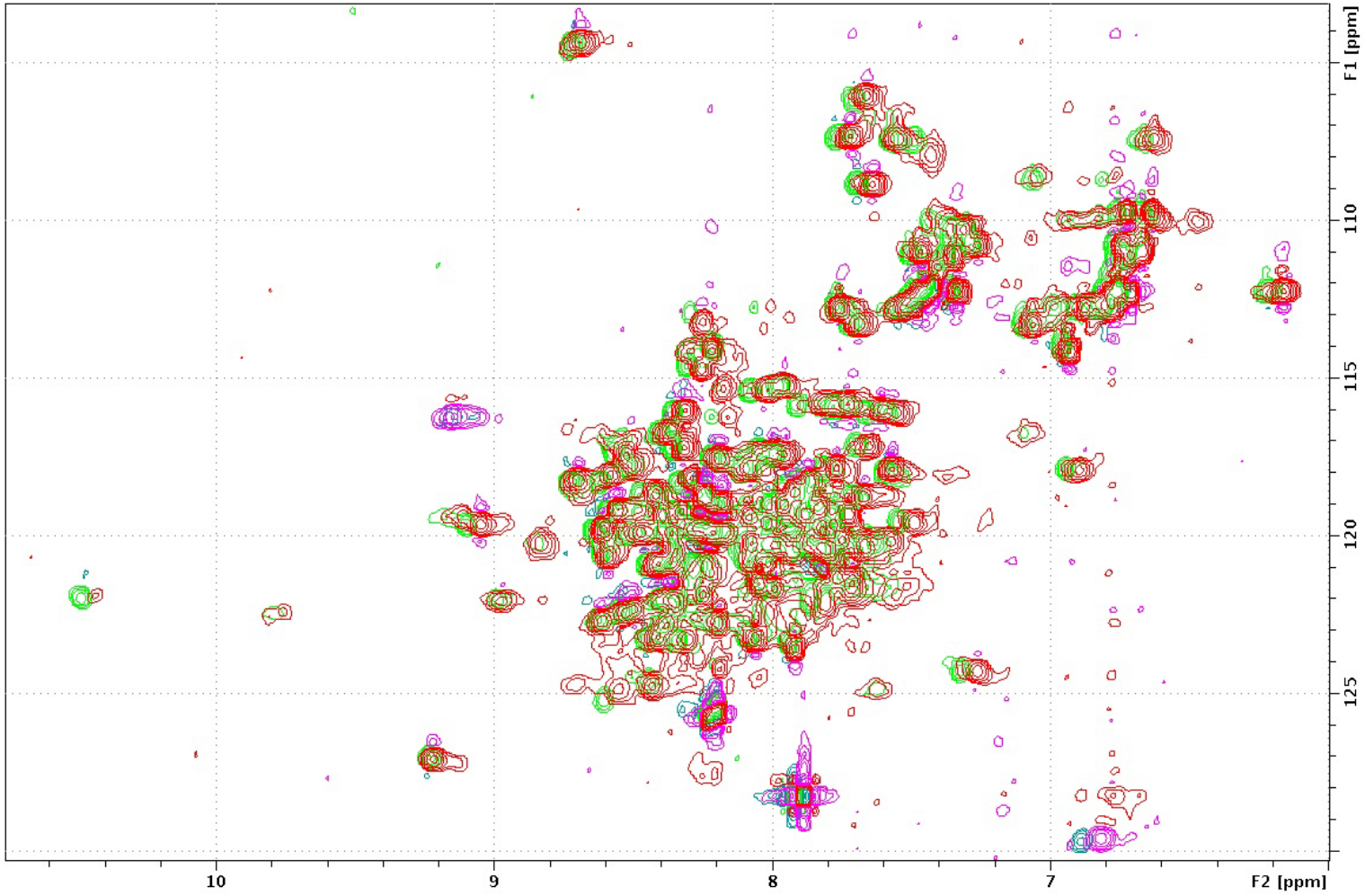

Himmel et al. Fig. S1b

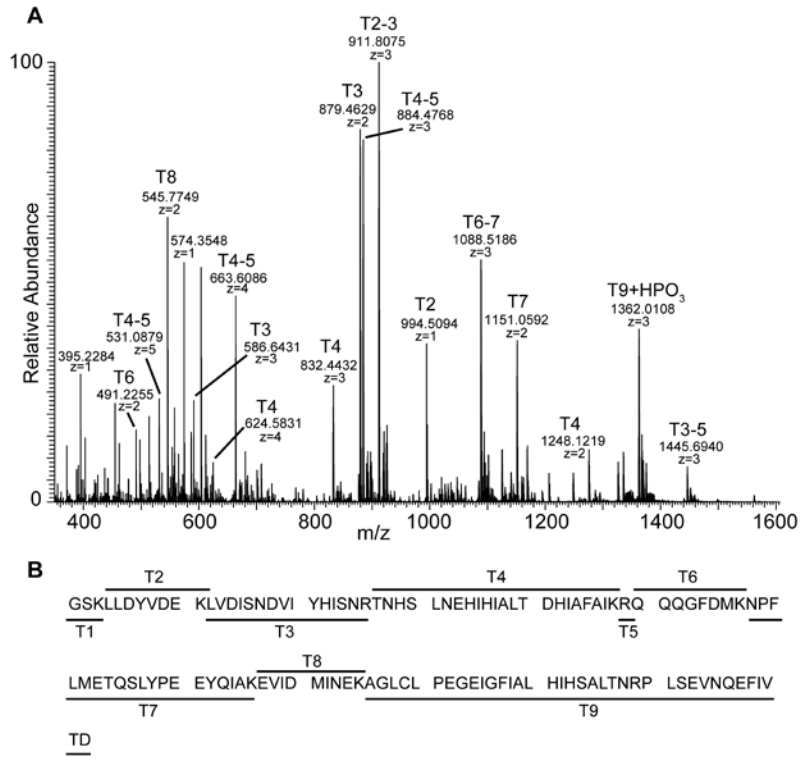

Himmel et al. Fig. S2

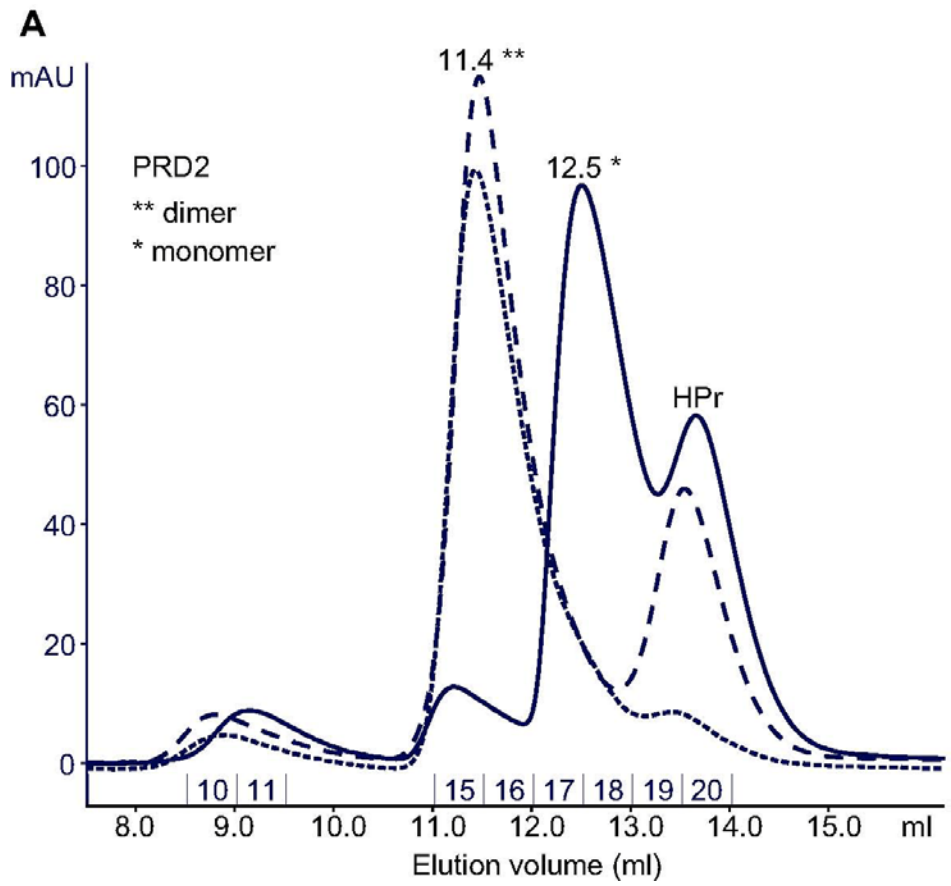

Himmel et al. Fig. S3

Himmel et al.

Legends to the Supplemental Figures

Fig. S1 HPr-dependent phosphorylation of PRD1 in the absence of Enzyme II investigated by NMR.
A. A $^{1}H,^{15}N$-HSQC spectrum of PRD1 shows the amide backbone resonances upon HPr-dependent phosphorylation. No Enzyme II was present in the phosphorylation mix. Positive and negative peak intensities are shown in black and green, respectively.
B Overlay of the spectra of Fig. 1E (red) and Fig. S1A(gray).

Fig. S2. ESI-MS analysis of tryptic PRD1 peptides.
A mass spectrum of tryptic PRD1 peptides was directly analyzed by ESI-Orbitrap MS (A) and returned a high protein sequence coverage 97.5%. Merely the tryptic peptide T1 (GSK) was not detectable owing to the out of m/z scan range from an Orbitrap MS analysis (B). The fragment ion of the dephosphorylated peak at m/z 1335.4 in a MS/MS spectrum (Fig 2) was subjected to a second ion isolation/fragmentation cycle (MS3) to obtain the information of peptide sequence AGLCLPEGEIGFIALHIHSALTNRPLSEVNQEFIVTD (C).

Fig. S3. Efficiency of HPr-dependent phosphorylation for PRD1 vs. PRD2 as studied by gel filtration chromatography.
The solid line indicates a 1:1 ratio of unphosphorylated PRD2/HPr, the long dashed line a 1:1 ratio of phosphorylated PRD2/HPr and the short dashed line indicates a 8:1 ratio of phosphorylated PRD2/HPr. These data clearly demonstrate the high efficiency of the phosphorylation of PRD2 by HPr, even at low HPr concentrations.